A beta2-frequency (20–30 Hz) oscillation in nonsynaptic networks of somatosensory cortex

Anita K. Roopun*, Steven J. Middleton*, Mark O. Cunningham*, Fiona E. N. LeBeau*, Andrea Bibbig†, Miles A. Whittington*, and Roger D. Traub†‡§

*Medical School, University of Newcastle, Newcastle NE2 4HH, United Kingdom; and Departments of †Physiology and Pharmacology and ‡Neurology, State University of New York Downstate Medical Center, Brooklyn, NY 11203

Communicated by Nancy J. Kopell, Boston University, Boston, MA, August 25, 2006 (received for review June 26, 2006)

Beta2 frequency (20–30 Hz) oscillations appear over somatosensory and motor cortices *in vivo* during motor preparation and can be coherent with muscle electrical activity. We describe a beta2 frequency oscillation occurring *in vitro* in networks of layer V pyramidal cells, the cells of origin of the corticospinal tract. This beta2 oscillation depends on gap junctional coupling, but it survives a cut through layer 4 and, hence, does not depend on apical dendritic electrogenesis. It also survives a blockade of α-amino-3-hydroxy-5-methyl-4-isoxazolepropionic acid receptors or a blockade of $GABA_A$ receptors that is sufficient to suppress gamma (30–70 Hz) oscillations in superficial cortical layers. The oscillation period is determined by the M type of K^+ current.

gap junction | intrinsic bursting | layer 5 | M current | neocortex

The mammalian neocortex generates a broad range of electroencephalogram rhythms concurrently in the awake behaving state. Some rhythms are strongly associated with sensory processing (the gamma band; ref. 1), whereas others are associated with cortical outputs (the beta band; ref. 2). Here we show an *in vitro* model of concurrent but independently generated gamma (30–70 Hz) rhythms in layer II/III and beta2 (20–30 Hz) rhythms in layer V somatosensory cortex. The beta2 rhythm occurred robustly in layer V intrinsically bursting (IB) neurons, in the form of bursts admixed with spikelets, and single action potentials. It was blocked by reducing gap junction conductance with carbenoxolone and was unaffected by blockade of synaptic transmission sufficient to ablate the layer II/III gamma rhythm. It also could be seen in the absence of synaptic transmission with axonal excitability enhanced with 4-aminopyridine, suggesting a nonsynaptic rhythm mediated by axonal excitation. A network model, based on the hypothesis of electrical coupling via axons, is consistent with this hypothesis. The frequency of this network beta2 rhythm was set by the magnitude of M current in IB neurons. Our data suggest the possibility that a normally occurring cortical network oscillation involved in motor control could be generated largely or entirely by nonsynaptic mechanisms.

Electroencephalogram beta oscillations, particularly those in the higher beta2 frequency range, have been recorded over premotor, supplementary motor, somatosensory, and other parietal cortical areas, in rats (3), monkeys (2, 4, 5), and humans (6). The oscillations are associated with sensory cues requiring sustained motor response and occur during the anticipatory period leading up to directed movement after such a sensory cue. The origin of these *in vivo* beta rhythms is unclear; however, pyramidal tract neurons (lying in layer V; ref. 7) and motor cortex local field potentials exhibit coherence at beta2 frequencies with hand and forearm electromyographic activity, in monkeys performing a precision grip task (8, 9), suggesting that beta2 oscillations originate in layer V *in vivo*. In addition, layer V neurons form a major input pathway to basal ganglia, which also demonstrate beta rhythms (10). Here, we demonstrate an *in vitro* model that shows that a beta2 rhythm (20–30 Hz) can be specifically generated in layer V of neocortex in a manner independent of gamma rhythmogenesis and of glutamatergic synaptic excitation. Beta2 generation in layer V stands in contrast to cortical gamma rhythms that have been shown to originate in layers II/III in *in vitro* models (11) and may underlie cortico-cortical synchronization (12).

Results

Recurrent glutamatergic activity in excitatory cortical networks has been shown to characterize active brain states (13, 14). These active states can be generated by kainate receptor-mediated activity alone in some areas of cortex (15), and exogenously applied kainate generates a persistent gamma frequency oscillation in all layers of auditory cortex (16). In contrast, in somatosensory cortex directly adjacent to auditory cortex (17), kainate application generated two distinct, coexistent frequencies of network rhythm. In superficial layers II/III, a gamma rhythm was observed (frequency 37.5 ± 4.5 Hz, power 556.2 ± 160.1 μV^2, $n = 6$), whereas in deep layers (V and VI), a beta2 frequency rhythm was observed (frequency 25.4 ± 3.2 Hz, power 396.2 ± 30.7 μV^2, $n = 6$; Fig. 1*A*). In layer IV, both rhythms were observed to coexist. To establish whether anatomically separate generator circuits were responsible for the two rhythms, a full-thickness cut of somatosensory cortical slices at the level of layer IV was used to completely physically separate layers I–III from layers V and VI (Fig. 1*B*). Gamma frequency field activity persisted in the superficial layers, with peak power in layer III, whereas beta2 frequency field activity persisted in the deep layers with peak power in layer V. These data indicate that the source of the beta2 frequency rhythm is anatomically and functionally separate from the superficial cortical layer gamma generator characterized in ref. 11.

To understand the mechanism of generation of layer V beta2 rhythms, we recorded from the somata of four main neuronal subtypes present in the deep layers. Layer V fast-spiking interneurons generated spikes on most beta2 periods (Fig. 4, which is published as supporting information on the PNAS web site). Both layer VI pyramids (Fig. 4) and layer V regular spiking neurons (data not shown) generated very low spike frequencies during beta2 rhythms (0.4 ± 0.1 and 1.1 ± 0.5 Hz, respectively) and had membrane potentials dominated by trains of inhibitory postsynaptic potentials at beta2 frequency. In contrast, layer V IB cells showed an unusual but highly robust (22 of 30 neurons recorded) pattern of activity, suggestive of being antidromically driven, consisting of intense barrages of spikelets and spikelet-bursts occurring at beta2 frequencies (Fig. 2 *A* and *B*); there were

Author contributions: A.K.R., M.O.C., F.E.N.L., M.A.W., and R.D.T. designed research; A.K.R., S.J.M., M.O.C., F.E.N.L., M.A.W., and R.D.T. performed research; A.K.R., S.J.M., M.O.C., F.E.N.L., A.B., M.A.W., and R.D.T. analyzed data; and M.A.W. and R.D.T. wrote the paper.

The authors declare no conflict of interest.

Freely available online through the PNAS open access option.

Abbreviations: AMPA, α-amino-3-hydroxy-5-methyl-4-isoxazolepropionic acid; IB, intrinsically bursting; RS, regular spiking.

§To whom correspondence should be addressed. E-mail: roger.traub@downstate.edu.

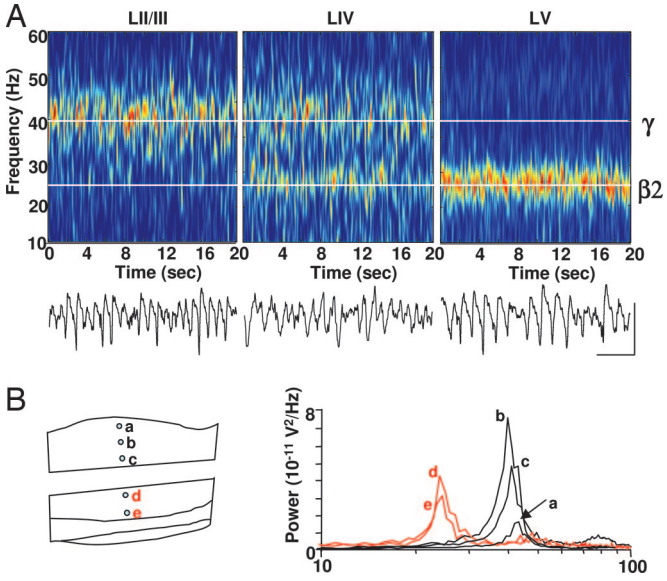

Fig. 1. Beta2 rhythms are generated in deep layers of cortex. (*A*) Spectrograms of field rhythms generated in somatosensory cortex slices by 400 nM kainate. Superficial layers generated gamma frequency (30–50 Hz) signals (layer II/III). Deep layers concurrently generated beta2 frequency signals (layer V, 20–30 Hz). Layer IV recordings show both frequency bands coexisting. Below each spectrogram are representative field potential traces (Scale bars: 0.2 mV, 100 ms). (*B*) Surgical separation of deep from superficial layers at the layer IV/V border abolished neither rhythm. Cartoon illustrates the electrode position for the power spectra taken from 60-s epochs of field potential data in the superficial layers (a–c, black lines) and deep layers (d and e, red lines).

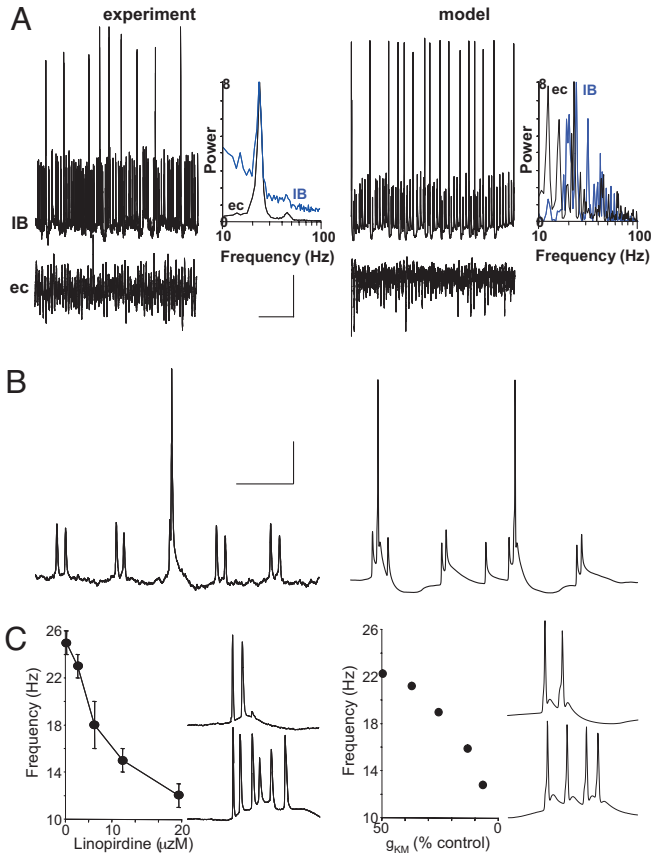

Fig. 2. Antidromic-appearing activity in LV IB cells predominates during beta2 rhythms. (*A Left*) Example trace (2.5-s) from an electrophysiologically and anatomically identified layer V IB cell reveals combinations of spikelets, single spikes, and spike bursts at beta2 frequencies (mean resting membrane potentials −55 mV). Power spectra show the frequency content of concurrently recorded IB cell (blue, IB) and layer V field (black, ec). (*A Right*) Field and tufted IB cell data are accurately predicted from antidromic spiking in model. (Scale bars: 10 mV, experiment intracellular; 100 μV, experiment field; 15 mV, model; 500 ms. (*B*) Expanded timescale examples of layer V IB cell activity during field beta rhythms. (Scale bars: 10 mV, experiment; 15 mV model; 10 ms.) (*C*) Beta2 frequency is correlated with $g_{K(M)}$-mediated control of burst duration. (*C Left*) Mean peak frequency ($n = 5$) of layer V field potentials. The decrease in population frequency with M current reduction (linopirdine 0–20 μM) was accompanied by increased IB cell burst duration. Examples are shown with 2 and 20 μM linopirdine. (*C Right*) Peak population frequency of model IB cells by using different $g_{K(M)}$ from 5% to 50% of control. Example bursts were taken with IB cell $g_{K(M)}$ = 50% and 5% of control. (Scale bars: 30 mV, experiment; 40 mV, model; 10 ms.)

occasional full somatic spikes/spike bursts generated off these spikelets (frequency 5 ± 2 Hz, Fig. 2*B*). Post hoc anatomical reconstruction of neurons displaying this activity revealed them to be tufted pyramidal neurons. Furthermore, this pattern of beta2 frequency spikelet/bursts also was observed in layer V neuronal somata after a cut through layer IV, indicating a non-apical-dendritic origin for this behavior. Computational modeling of a network of realistic 61-compartment IB neurons predicted that this pattern of beta2 frequency antidromic activity could be generated by ectopic action potential generation in the model plexus of IB neuronal axons interconnected by axo-axonic gap junctions (Fig. 2 *A* and *B*). The model predicted that the beta2 periodicity came primarily from the presence of M current in pyramidal cell axons and somata (18). We tested this prediction by bath application of increasing concentrations of the M current blocker linopirdine (2–20 μM; ref. 19). In both the model and experiment, reduction in M current reduced beta2 field potential frequency and increased the duration of burst discharges seen in IB neuronal somata (Fig. 2*C*).

The prediction that the layer V beta2 generating network did not require phasic synaptic input was tested by using pharmacological blockade of the main components of glutamatergic and GABAergic transmission in the cortex. It has been shown that the superficial layer gamma rhythm generator critically depends on α-amino-3-hydroxy-5-methyl-4-isoxazolepropionic acid (AMPA) receptor-mediated phasic drive to interneurons (11) and an NMDA receptor mediated tonic drive to specific subpopulations of interneuron (20). Therefore, recording of concurrent gamma and beta2 rhythms in layer IV should reveal a selective effect of blockers of these glutamate receptor subtypes on the gamma rhythm. Bath application of the AMPA receptor blocker SYM2206 (20 μM), which preserves the kainate receptor-mediated component of the kainate drive, abolished the modal peak in the gamma frequency band and significantly reduced overall power in this band ($P < 0.05$, $n = 6$). The coexpressed beta2 rhythm was unaffected in power or modal peak frequency by AMPA receptor blockade ($P > 0.05$, $n = 6$). A similar selective effect of NMDA receptor blockade also was seen. D-AP5 (50 μM) abolished the gamma band peak in layer IV power spectra but caused a significant increase in peak power in the beta2 frequency band ($P < 0.05$, $n = 6$; Fig. 5, which is published as supporting information on the PNAS web site).

The superficial gamma rhythm also has been shown to be depend critically on $GABA_A$ receptor-mediated phasic inhibition of layer II/III principal cells (11). We tested two concentrations of the selective $GABA_A$ receptor blocker gabazine (Fig. 5). At 250 nM, gabazine abolished the spectral peak in the gamma band but doubled the mean amplitude of the beta2 peak ($P < 0.05$, $n = 6$) with no change in modal peak frequency ($P > 0.05$). However, at higher concentrations (2 μM, $n = 6$), gabazine abolished all rhythmic activity and precipitated spontaneous

NEUROSCIENCE

interictal-like bursts (incidence 0.43 ± 0.05 s^{-1}), suggesting some dependence on GABA activity to maintain the antidromic beta2 rhythm, perhaps via depolarization of principal cell axon initial segments (21). These data suggest a complex relationship between beta2 rhythm-generating circuits and $GABA_A$ receptor-mediated synaptic effects, which did not involve conventional perisomatic feedback inhibition as seen for gamma rhythms. The $GABA_B$ receptor antagonist CGP55845 (10 μM, $n = 6$) had no significant effect on either gamma or beta2 frequency rhythms.

The antidromic-appearing, largely nonsynaptic nature of the layer V beta2 rhythm was examined further by using gap junction-blocking drugs. The model simulations predicted that, if ectopic spikes provided the main driving force for the generation of the rhythm, then conduction of these spikes through gap junctions forming an axonal plexus would be a critical component of the mechanism. Dye coupling within layer V neuron populations has been observed in adult cortex (22) and the huge incidence of spikelets, associated with axo-axonic dye coupling and gap junctional communication in hippocampus (23–24), suggested such a mechanism possibly may underlie the beta2 rhythm. Both octanol (1 mM, data not shown) and carbenoxolone (0.2 mM, Fig. 3*A*), drugs that each are capable of reducing gap junction conductance, abolished beta2 field potential activity. In both the experiment and model, some spikelets and antidromically elicited somatic spikes remained (Fig. 3*A*), suggesting that ectopic spike generation remained active, but that intercellular distribution of these events via gap junctions was absent, leading to a collapse of the locally synchronous beta2 rhythm.

All of the above lines of evidence point to a mechanism for beta2 rhythmogenesis involving antidromic activity propagating through axo-somatic compartments of layer V IB neurons. However, the suggestion that $GABA_A$ receptors may provide an excitatory drive to axons (20) and the partial ionotropic nature of kainate-mediated synaptic principal cell excitation needed to be addressed. If a beta2 rhythm were to be generated in the absence of all synaptic activity (including the original kainate receptor-mediated drive), the model predicted that a source of excitation targeting intrinsic axonal conductances would be required experimentally. 4-aminopyridine has been shown to increase axonal excitability and potentiate antidromic spiking (25, 26) so we applied 4-aminopyridine to sensorimotor cortical slices in the presence of blockers for AMPA, NMDA, kainate, $GABA_A$, and $GABA_B$ receptors. Transient (2–30 s) epochs of beta2 field potential activity were observed in layer V (Fig. 3*B*, $n = 5$ slices). The resulting field potentials were less sinusoidal than the kainate-induced rhythm, with a greater degree of multiunit activity evident. However, the pattern of IB cell spiking and the mean frequency of the field corresponded well to the beta2 rhythm induced with intact cortical connectivity, and the population oscillation also was not seen in the presence of carbenoxolone (data not shown). Network simulations also showed the presence of the beta2 oscillation when chemical synapses were blocked and axonal excitability was increased (Fig. 3*B*).

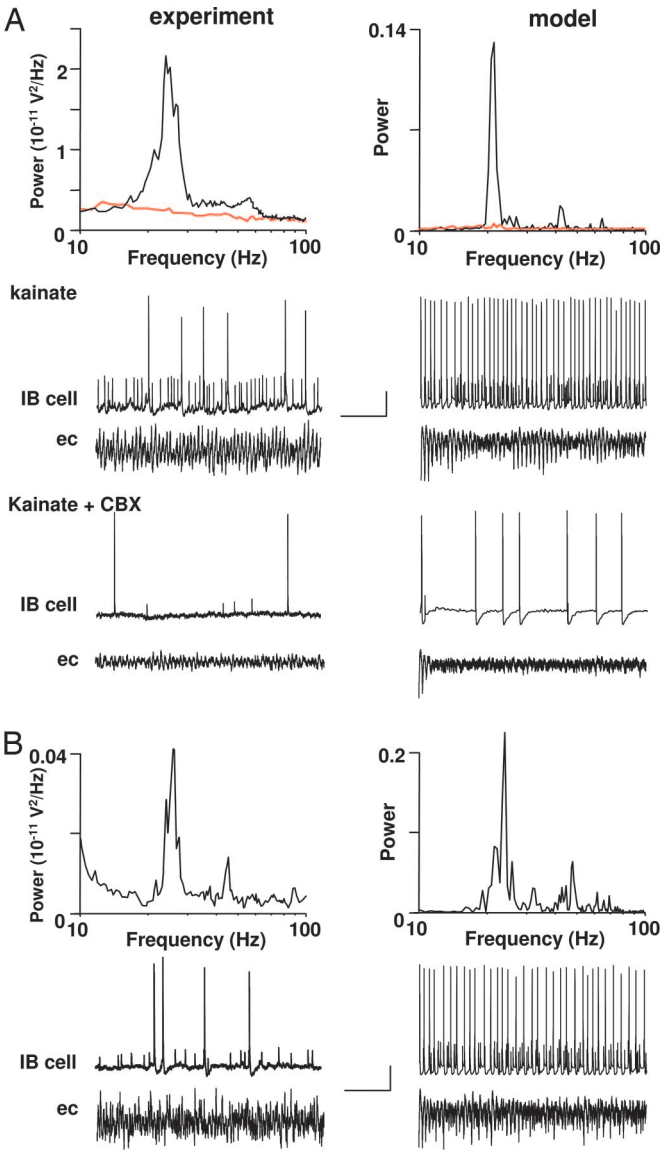

Fig. 3. Beta2 rhythms in nonsynaptic networks of IB cells. (*A Left*) Mean power spectra derived from 60-s epochs of oscillation from layer V field potentials ($n = 5$) showed blockade of beta2 activity by the gap junction blocker carbenoxolone (control, black; 0.2 mM carbenoxolone, red). Example traces show layer V beta2 activity (ec) and antidromic-appearing activity in an IB cell (IB) before and 1 h after carbenoxolone. (*A Right*) Corresponding model spectra and IB activity in the presence (black line) and absence (red line) of gap junctional conductances. (Scale bars: 20 mV, experiment; 25 mV, model; 0.5 s.) (*B Left*) Beta2 rhythms can be elicited in the absence of the main fast excitatory and inhibitory synaptic transmission pathways. Experimental data shows mean power spectrum (derived from $n = 5$, 2-s epochs of data) of layer V population activity in the presence of blockers for AMPA, kainate, NMDA, and GABA receptors (20 μM NBQX, 50 μM dAP5, 20 μM bicuculline, and 10 μM CGP55845); there was also bath application of 4-aminopyridine (40 μM) to increase neuronal excitability, compensating for the blockade of the original kainate receptor-mediated drive. Example traces show that, in these nonsynaptic conditions, activity is dominated by antidromically appearing full and partial spikes in IB cells. (*B Right*) The model can reproduce this beta2 rhythm accurately in the absence of synaptic conductances, when axonal R_m is doubled. The model full and partial spikes indeed are antidromic. (Scale bars: 20 mV, experiment; 25 mV, model; 500 ms.)

Discussion

The occurrence of cortical beta2 rhythms is associated with stable states in the *in vivo*-behaving motor system: during anticipation, motor preparation, and sustained activity during stereotyped motor output. We have shown that a similar rhythm can be generated *in vitro*, independently from gamma rhythms, in nonsynaptic networks of layer V-bursting neurons activated by kainate and, perhaps, $GABA_A$ receptors (e.g., ref. 21). With concentrations of $GABA_A$ receptor antagonist, sufficient to abolish gamma rhythms, beta2 rhythms were enhanced. Higher concentrations abolished beta2 rhythms, but it is unclear as yet whether this effect was a consequence of selective actions on subsets of inhibitory synapses or whether the effect was an indirect consequence of the epileptiform activity observed (e.g., suppression of depolarization via postburst AHPs or gap junc-

tion blockade as a consequence of burst-induced intracellular calcium rises). Unlike persistent gamma rhythms, which have an absolute requirement for phasic synaptic excitation and inhibition, beta2 rhythms may represent a developmentally preserved, primary operational mode of the neocortex, being modified by, but not absolutely dependent on, synaptic activity in the mature brain. These data suggest that this rhythm is present to functionally separate activity in superficial cortical layers (gamma) from output pathways in deep layers (beta2). Our data also suggest that mature cortex can express forms of network behavior, primarily dependent on gap junctional coupling, that are usually associated with the immature, developing, nervous system (27).

Materials and Methods

Simulation Methods. We used a network model derived from ref. 16: We retained the cells in deep cortical layers and omitted cells in layers 2, 3, and 4 and thalamic cells. Modifications were made in the number of cells used and the intrinsic membrane properties, and these modifications are described below. Individual neurons were multicompartment objects with soma, branching dendrites, and a short axon. Each compartment contained up to 11 different active membrane conductances. Network simulations were run on 22 central processing units of an IBM e1350 Linux cluster. Parallel code was written in Fortran, augmented by MPI instructions for a parallel computing environment.

The numbers of cells used in the present simulations were as follows: 2,000 layer V tufted pyramidal cells with IB properties, the main contributors to network behavior considered herein; 200 layer V tufted pyramids with regular spiking (RS) firing behavior; 500 nontufted layer 6 RS pyramidal neurons; 100 fast-spiking basket interneurons; 100 fast-spiking axoaxonic interneurons; and 100 low-threshold spiking dendrite-contacting interneurons.

Intrinsic properties were altered from the original study (16) mainly in the properties of the axons of the pyramidal neurons. In the original study (16), the density of transient Na^+ conductance was significantly higher in the axon than the soma but with identical kinetics. Now we use the same density in the axon as the soma (28) but shift the activation kinetics to the left in the axon: by 5 mV in tufted IB pyramids (with a range of 0–10 mV tried) and by 7 mV in other pyramidal cells. In addition, the shape of burst after-potentials forced us to shift V_K (the equilibrium potential for K^+ currents) from -95 mV to -85 mV in tufted IB pyramidal cells. We found that simulated network bursts at beta frequency did not require high-threshold Ca^{2+} conductance, so this conductance was reduced at least 10-fold in each tufted IB pyramidal cell; that manipulation had the effect of reducing Ca^{2+}-dependent K^+ currents. Finally, the tufted IB pyramidal cells were randomly biased by injecting a current into each basal and oblique dendritic compartment of -0.02 to $+0.02$ nA. Random noise was present in the form of spontaneous action potentials in the axons of pyramidal cells, Poisson-distributed, at means of 4 Hz per axon for tufted IB pyramidal cells and 1 Hz per axon for other pyramidal cells.

Chemical synaptic connectivity was as in the original study (16). Some of the parameters were as follows: each tufted IB pyramid had synaptic input from 50 IB pyramids and 20 basket cells; each basket cell had input from 20 IB pyramids and 20 basket cells; and each tufted RS pyramid and each nontufted RS pyramid had input from 20 IB pyramids and 20 basket cells. "Baseline" scaling factors for IB pyramid AMPA conductances were 2 nS in pyramidal cells and 3 nS in basket cells. AMPA receptor-mediated conductances were proportional to an alpha function, with a time constant of 2 ms in pyramidal cells, 0.8 ms in fast-spiking interneurons, and 1.0 ms in low-threshold spiking interneurons. $GABA_A$-receptor-mediated conductances rose instantaneously and decayed exponentially, with a time constant of 6 ms in pyramidal cells, and 3 ms in interneurons when induced by basket cell firing, but with a time constant of 20 ms when induced by low-threshold spiking interneuron firing. The unitary basket cell-induced conductance (in baseline simulations) peaked at 0.07 nS in pyramidal cells and 0.2 nS in basket cells, with a wide range of possible conductances explored. Axon conduction delays were ignored.

The average number of gap junctions on an IB pyramidal cell axon, coupling to another tufted IB pyramidal cell axon, was 2. The corresponding number for tufted RS pyramids was 1.6 and for nontufted RS pyramids was 2. In addition, a few (total 50) gap junctions in the network interconnected tufted IB/tufted RS pyramidal cell pairs. Gap junction conductances were 4.0–4.5 nS, enough to allow an action potential to cross from axon to axon (29). The gap junctions were located on the most distal axonal compartment of each pyramidal cell model, centered 150 μm from the soma. The existence and properties of these model gap junctions constitute a basic hypothesis of our model.

Experimental Methods. Horizontal slices (450-μm thick) were prepared from adult male Wistar rats (150–250 g). Neocortical slices containing auditory areas and secondary somatosensory cortical areas were maintained at 34°C at the interface between warm wetted 95% O_2/5% CO_2 and artificial cerebrospinal fluid (aCSF) containing 3 mM KCl, 1.25 mM NaH_2PO_4, 1 mM $MgSO_4$, 1.2 mM $CaCl_2$, 24 mM $NaHCO_3$, 10 mM glucose, and 126 mM NaCl. Extracellular recordings from somatosensory cortex were obtained by using glass micropipettes containing the above aCSF (resistance <0.5 MΩ). Intracellular recordings were taken with sharp microelectrodes filled with potassium acetate (resistance 30–90 MΩ). Signals were analog filtered at 2 kHz and digitized at 10 kHz. All neuronal recordings illustrated were taken from layer V, unless stated otherwise. Power spectra were taken from 60-s epochs of data except in the case of beta2 rhythms generated in nonsynaptic conditions. Here, the rhythm occurred in transient epochs, so a window of only 2 s was used to allow pooling of data across multiple slices/experiments.

This work is dedicated to the memory of Mircea Steriade. We thank Nancy Kopell for discussions. This work was supported by the Medical Research Council (U.K.), the Wellcome Trust, and the National Institutes of Health.

1. Gray CM, Singer W (1989) *Proc Natl Acad Sci USA* 86:1698–1702.
2. MacKay WA, Mendonça AJ (1995) *Brain Res* 704:167–174.
3. Hamada Y, Miyashita E, Tanaka H (1999) *Neuroscience* 88:667–671.
4. Lebedev MA, Wise SP (2000) *Exp Brain Res* 130:195–215.
5. Lee D (2003) *J Neurosci* 23:6798–6809.
6. Wheaton LA, Shibasaki H, Hallett M (2005) *Clin Neurophysiol* 116:1201–1212.
7. Toyoshima K, Sakai H (1982) *J Hirnforsch* 23:257–269.
8. Baker SN, Olivier E, Lemon RN (1997) *J Physiol* 501:225–241.
9. Baker SN, Kilner JM, Pinches EM, Lemon RN (1999) *Exp Brain Res* 128:109–117.
10. Courtemanche R, Fujii N, Graybiel AM (2003) *J Neurosci* 23:11741–11752.
11. Cunningham MO, Whittington MA, Bibbig A, Roopun A, LeBeau FEN, Vogt A, Monyer H, Buhl EH, Traub RD (2004) *Proc Natl Acad Sci USA* 101:7152–7157.
12. Rodriguez E, George N, Lachaux, J-P, Martinerie J, Renault B, Varela FJ (1999) *Nature* 397:430–433.
13. Steriade M, Contreras D, Amzica F, Timofeev I (1996) *J Neurosci* 16:2788–2808.
14. Steriade M (2000) *Neuroscience* 101:243–276.
15. Cunningham MO, Pervouchine DD, Racca C, Kopell NJ, Davies CH, Jones RSG, Traub RD, Whittington MA (2006) *Proc Natl Acad Sci USA* 103:5597–5601.
16. Traub RD, Contreras D, Cunningham MO, Murray H, LeBeau FEN, Roopun A, Bibbig A, Wilent WB, Higley MJ, Whittington MA (2005) *J Neurophysiol* 93:2194–2232.
17. Paxinos G, Watson C (2004) *The Rat Brain in Stereotaxic Coordinates* (Elsevier, Amsterdam).

18. Cooper EC, Harrington E, Jan YN, Jan LY (2001) *J Neurosci* 21:9529–9540.
19. Wang HS, Pan Z, Shi W, Brown BS, Wymore RS, Cohen IS, Dixon JE, McKinnon D (1998) *Science* 282:1890–1993.
20. Cunningham MO, Hunt J, Middleton S, LeBeau FEN, Gillies MJ, Davies CH, Maycox PR, Whittington MA, Racca C (2006) *J Neurosci* 26:2767–2776.
21. Szabadics J, Varga C, Molnár G, Oláh S, Barzó, P & Tamás G (2006) *Science* 311:233–235.
22. Gutnick MJ, Lobel-Yaakov R, Rimon G (1985) *Neuroscience* 15:659–666.
23. Draguhn A, Traub RD, Schmitz D, Jefferys JGR (1998) *Nature* 394:189–192.
24. Schmitz D, Schuchmann S, Fisahn A, Draguhn A, Buhl EH, Petrasch-Parwez E, Dermietzel R, Heinemann U, Traub RD (2001) *Neuron* 31:831–840.
25. Preston RJ, Waxman SG, Kocsis JD (1983) *Exp Neurol* 79:808–820.
26. Traub RD, Colling SB, Jefferys JGR (1995) *J Physiol* 489:127–140.
27. Dupont E, Hanganu IL, Kilb W, Hirsch S, Luhmann HJ (2006) *Nature* 439:79–83.
28. Colbert CM, Pan E (2002) *Nat Neurosci* 5:533–538.
29. Traub RD, Schmitz D, Jefferys JG, Draguhn A (1999) *Neuroscience* 92: 407–426.